研究ノート

Electronic Properties of Cryogenic Rare Gas Liquids and Their Applications in Radiation Detectors

Graduate School of Engineering Werner F. Schmidt、Katsumi Yoshino (Ext. 7757)

E-mail: yoshino @ele.eng.osaka-u.ac.jp

Abstract

Cryogenic liquids find many applications in science and technology. Here, an overview of the electronic properties of liquefied rare gases is given. Their application as ionization media in radiation detectors is discussed.

1. Introduction

The detection of ionizing radiation has great importance in science and technology. From the early use of air ionization chambers and Geiger-Mueller-counters the modern development of radiation detectors encompasses gases, liquids, and solids as ionization media. Especially, the construction of high energy physics experiments employing big accelerators or cosmic ray detection in underground laboratories has spurred the use of a variety of gases and solids. The application of liquids up to the present time is more restricted. On one hand this stems from a lack of understanding of the basic electronic properties of many possible candidates and on the other hand from the fact that liquids usually are associated with chemistry rather than physics, which leads to a reluctancy on the part of physicist to explore the possibilities of liquids. One exeption are the rare gas liquids which are being used on a large scale in the construction of radiation detection systems for high energy physics research.

In this short review we discuss the electronic properties of rare gas liquids (RGL) and we describe some examples of their use in experiments of detection of elementary particles and high energy photons.

2. Thermo-Physical Properties

Some thermo-physical properties of RGLs are summarized in Tables 1 and 2. The heavier RGL are examples of classical, non-polar dielectric liquids. lHe and partly also lNe exhibit quantum properties. One consequence is the absence of a melting point for lHe. Under orthobaric conditions it remains liquid down to the lowest temperatures. The solid phase of He can only be observed under application of external pressure ($>$ 29 bar at 4.2K).

Liquid xenon has the widest liquid range, its critical point is at 16.6 ℃, which has made it to a prominent solvent in chemistry [2].

The rare gases -except helium- are produced in the liquefaction of air. The application of RGLs is a growing market; in the future, the demand for xenon by high energy physics and by medecine may outstrip the available resources [4].

Table 1: Properties of rare gas liquids; Nel number of electrons per atomolecule; nel electrons per cc [1]

	T_{bp}[K]	ρ_{bp}[g/cm^3]	T_c [K]	p_c [bar]	T_{trp} [K]	V_{gas}/V_{liq}*)	Nel	n_{bp} [cm^{-3}]	n_{el} [cm^{-3}]
He	4 .22	0.125	5.21	2.27		748	2	1.88 10^{22}	3.76 10^{22}
Ne	27.10	1.207	44.41	27.56	24.55	1434	10	3.62 10^{22}	3.62 10^{23}
Ar	87.29	1.393	150.86	48.98	83.78	836	18	2.09 10^{22}	3.76 10^{23}
Kr	119.80	2.413	209.41	55.02	115.95	688	36	1.73 10^{22}	6.51 10^{23}
Xe	165.03	3.057	289.75	58.40	161.35	550	54	1.40 10^{22}	7.56 10^{23}

*) V_{gas} at 15^{0}C and 1 bar, V_{liq} at T_{bp}.

Table 2: Triple point properties of rare gas liquids; V in cm^3/mole [3]

	T_{trp} [K]	p_{trp} (Torr)	V_{gas}	V_{liq}	V_{sol}
Ne	24.55	325	4600	16.18	14.06
Ar	83.81	517	9867	28.24	24.63
Kr	115.76	547	12850	34.32	30.01
Xe	161.39	612	16050	44.31	38.59

3. Dielectric Properties

An important physical quantity in all applications of liquids is the relative dielectric constant. The RGLs can be considered as model liquids for the use of the Clausius-Mossotti equation. To a good approximation, the relation of the dielectric constant of a liquid, ε_r, to its density, ρ, is given by [5],

$$\frac{\varepsilon_r - 1}{\varepsilon_r + 2} = C\,\rho \tag{1}$$

or

$$\varepsilon_r - 1 = \frac{3C\rho}{1 - C\rho} \tag{2}$$

where C is a constant determined by the polarizability, α_{pol}, of the atoms comprising the liquid. For RGLs, the C-M-equation becomes,

$$\frac{\varepsilon_r - 1}{\varepsilon_r + 2} = \frac{1}{3\varepsilon_0}\,\frac{\rho N_A}{M}\,\alpha_{pol} \tag{3}$$

M is the molecular or atomic weight, N_A is Avogadro's number. α_{pol} is in Fm^2; (in electrostatic units, α_{pol} is given in cm^3). Conversion between the two systems of units is obtained by multiplying α_{pol} (esu) by 1.1127x10^{-16}. The variation of the dielectric constant with density is obtained as,

$$\rho\frac{\partial \varepsilon_r}{\partial \rho} = \frac{\varepsilon_0}{3}(\varepsilon_r - 1)(\varepsilon_r + 2) \tag{4}$$

The C-M-equation can be used to calculate the dielectric constants of RGLs from gas phase polarizabilities. In Fig. 1, calculated dielectric constants of xenon are compared with measured values.

The polarizability of the rare gas atoms increases with the number of electrons in their shells and the dielectric constant of the RGLs increases in addition with the density of the li-

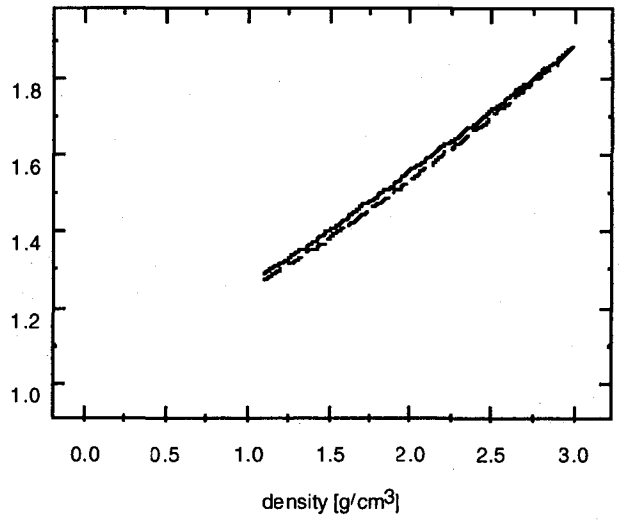

Fig. 1: Dielectric constant of liquid xenon [6] ; [7] ; [8]

quid. Data of ε_r are compiled in Table 3.

Table 3: Dielectric constants of RGLs [9] ; [10] ; [11] ; [12] ; [8]

liquid	symbol	T[K]	ε_r
helium	^{4}He	4.2	1.05
neon	Ne	27.1	1.18
argon	Ar	85	1.51
krypton	Kr	117	1.66
xenon	Xe	162	1.92_5

The low dielectric constant of lHe is due to the low polarizability of the He atom. The two K-electrons are tightly bound to the nucleus and their orbits cannot be shifted much by an external electric field. In addition, the density of lHe is small.

4. Electronic Energy Levels

The energy band model of electronic energy levels was developed for crystalline solids. Condensation of atoms into a regular spatial arrangement of long range order, the crystal lattice, leads to the formation of new energy levels of the valence electrons due to the action of the Pauli exclusion principle. These electronic levels form the valence band. The ionization continuum of the isolated atoms is replaced by the conduction band in the solid.

For the description of the electronic energy levels of RGLs, we use the band model. The adaptation of this model needs some justification since the RGLs are characterized by a lack of long range spatial order.

The electron mobility in solid argon, krypton, and xenon decreases roughly by a factor of two at the melting point [13]. Experiments on clusters of metals, semiconductors, and insulators show that a condensate of several tens or hundreds of atoms exhibits already the electronic properties of the macroscopic crystalline solid [14] , [15] . Gubanov [16] demonstrated that the description of the electronic energy levels of a crystalline solid by the Schrödinger equation can be maintained when fluctuations in the periodicity of the lattice are introduced.

The RGLs are insulators from a physical point of view. In Fig. 2 the change of energy levels of an atom upon condensation is depicted, schematically. A filled valence band and an

empty conduction band are formed. In the liquefied rare gases both bands are probably several eV in width as can be estimated from measurements of the solid rare gases.

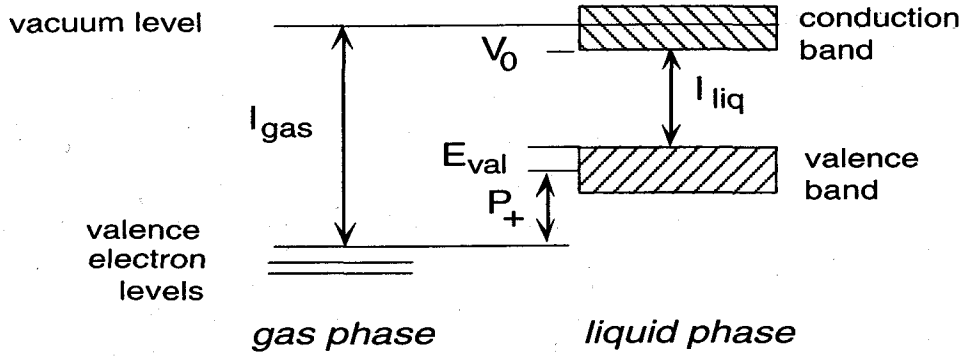

Fig 2: Change of electronic energy levels upon condensation

The symbols denote the following physical quantities: I_{gas} gas phase ionization energy, I_{liq} ionization energy in the liquid phase, P_+ polarization energy of the positive ion, V_0 energy of the electronic conduction level (bottom of the conduction band), E_{val} shift of the valence levels.

Values of V_0, I_{gas}, and I_{liq} have been measured and P_+ can be estimated from the following relationship,

$$I_{liq} = I_{gas} + V_0 + P_+ + E_{val} \tag{5}$$

V_0, P_+ and E_{val} are negative values if the energy of the vacuum level is set to be zero. $E_{val} \approx 0.1$ eV has been estimated from photo electron spectra of solids. It is usually neglected. In Table 4 measured values are compiled.

Table 4: Ionization energies and V_0 -values in eV [17]

liquid	I_{gas}	I_{liq}	V_0
helium	24.46	n.a.	+ 1.05
neon	21.47	n.a.	+ 0.67
argon	15.68	n.a.	- 0.20
krypton	13.93	11.56	- 0.40
xenon	12.08	9.2	- 0.67

I_{liq} - values for lAr, lNe, and lHe can be estimated, since the polarization energy of the positive charge P + can be estimated by a formula derived by Born [18],

$$P_+ = -\frac{e_0^2}{8\pi\varepsilon_0 R}\left[1 - \frac{1}{\varepsilon_r}\right] \tag{6}$$

ε_0 denotes the permittivty of free space, ε_r is the relative dielectric constant, and R denotes the radius of the ion.

5. Thermal Excitation of Electron-Hole Pairs

Thermal excitation of charge carriers is related to I_{liq}. For pure, crystalline insulators the concentration of electron/hole pairs, n (m^{-3}) due to thermal ionization has been derived as [19],

$$n = 2\left[\frac{2\pi k_B T}{h^2}\right]^{3/2} (m_{el}^* m_h^*)^{3/4} \exp\left(-\frac{I_{liq}}{2k_B T}\right) \tag{7a}$$

Here m_{el}^* and m_h^* are the effective masses of the electron and hole, respectively. For an estimate of the intrinsic charge carrier concentration, n, in a RGL, we assume the effective

masses of electron and hole to be equal to that of the free electron ($0.91\ 10^{-30}$ kg). Equation 7a then becomes

$$n\ [m^{-3}] = 4.83\ 10^{21} T^{3/2} \exp\left(-\frac{I_{liq}}{2k_B T}\right) \tag{7b}$$

Taking values for I_{liq} given in Table 4, values for n are obtained which indicate that in the liquefied rare gases no thermal excitation of electron pairs takes place. RGLs are excellent electric insulators from a physical point of view.

Application of very high pressures leads to a stronger interaction of the valence electron shells and a broadening of the electronic bands. A reduction of the band gap results. Solid xenon under a static pressure of ps $\geq$ 33 GPa loses its insulating properties and becomes a conductor [20]. The electrical conductivity changes over 9 orders of magnitude (see Fig. 3).

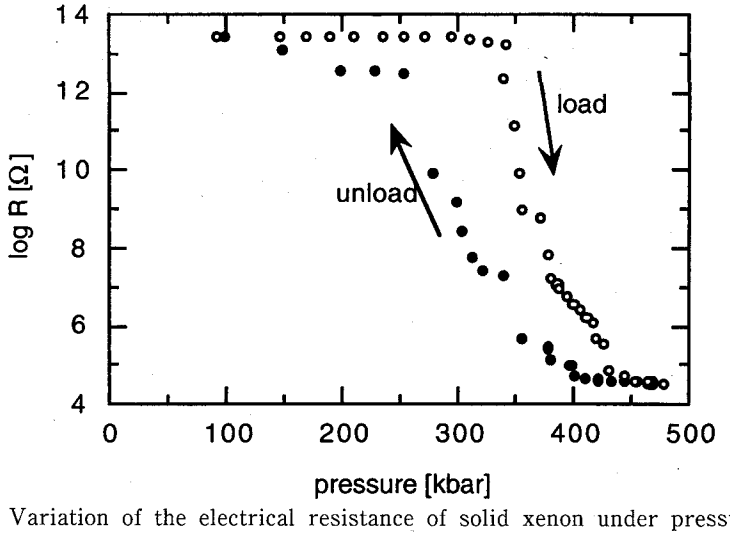

Fig. 3: Variation of the electrical resistance of solid xenon under pressure [20]

6. Injection of Excess Charge Carriers in RGLs

Excess charge carriers in RGLs have to be introduced by external agents. The most prominent ones are summarized in the following list.

Injection of electrons, holes and ions in non-polar dielectric liquids

Ionization by high energy radiation
x-rays
fast electrons
UV-light
elementary particles
laser-induced multi-photon absorption

Photoelectric emission from metal or semiconductor cathodes

Field emission or field ionization at tips or blades

Injection from the gas phase
low pressure discharge
glow cathode

Semiconductor diodes

Streaming liquids

Ionizing radiation produces negative and positive charge carriers at the same time. Some other methods are used when one kind of charge carrier is to be studied only. These injection methods are combined with a suitable geometry of the experimental test cell for the measurement of the energetics or dynamics of excess charge carriers.

7. Electron Mobility

The RGLs fall into two classes with respect to their electron mobility. In liquid helium and neon, near the boiling point, the electron mobility is much smaller than $1 cm^2 V^{-1} s^{-1}$. The charge carrier is depicted as a bubble of 10 to 20 Å radius occupied by the electron. In lAr, lKr, and lXe the electron mobility is much higher (see Table 5). In the

Table 5: Electron mobility and saturation velocity in liquefied rare gases [21] ; [22]

liquid	T[K]	μ_{el} [$cm^2V^{-1}s^{-1}$]	v_s [$cm\ s^{-1}$]
Helium	4.2	$2\ 10^{-2}$	
Ne	25	$1.6\ 10^{-3}$	
	25	(200 - 300)*	10^6
Ar	87	400±50	$6.4\ 10^5$
	85	475	$7.5\ 10^5$
	85	625±15	$(9.1\pm0.3)\ 10^5$
	87		$6\ 10^5$
	87		$8\ 10^5$
Kr	120	1200±150	$4.5\ 10^5$
	117	1800	$3.8\ 10^5$
	119		$3.3\ 10^5$
	120.4	1310	
Xe	165	2000±200	$2.6\ 10^5$
	163	1900	$2.9\ 10^5$
	167	1100	
	165	2950±50	$2.95\ 10^5$

*) mobility of delocalized electrons estimated from the mobility in solid neon of ≈ 600 $cm^2V^{-1}s^{-1}$ [23]

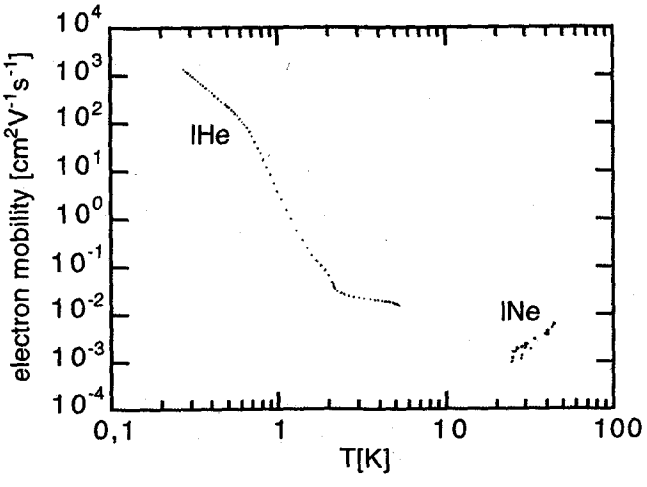

Fig. 4: Electron mobility in lHe [24] and lNe [25] ; [21] as a function of temperature

latter liquids, electron transport is thought to occur in the delocalized state (conduction band).

The temperature dependence of the mobility in liquid helium and liquid neon is depicted in Fig. 4. In lHe, μ_{el} increases with decreasing temperature. The strong increase below 2.1 K is due to the appearance of the superfluidity. In liquid neon the mobility is thermally activated up to the critical temperature. In both liquids, the drift mobility is independent of the electric field strength up to about 60kV/cm, the highest value employed [26] ; [27] ; [21]

Liquid neon is an especially interesting liquid since both quasifree and localized electrons

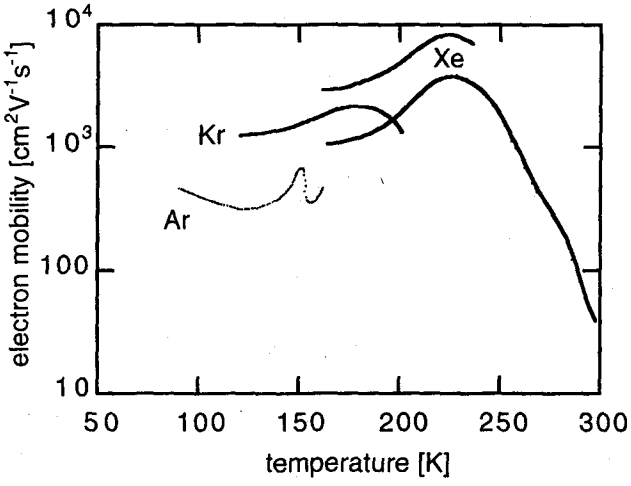

Fig. 5: Electron mobility in liquid Ar, Kr, and Xe as a function of temperature [28] [29]

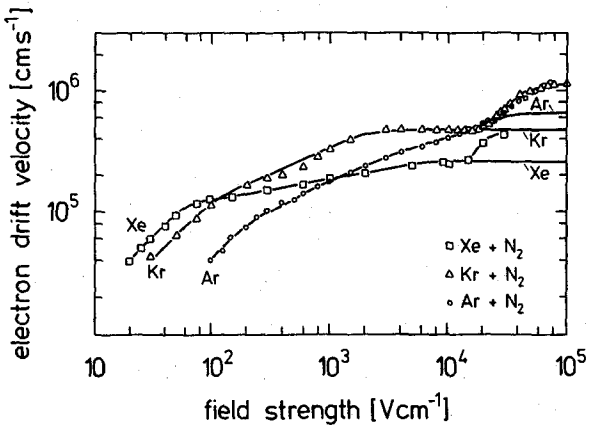

Fig. 6: Drift velocity as a function of electric field [30]

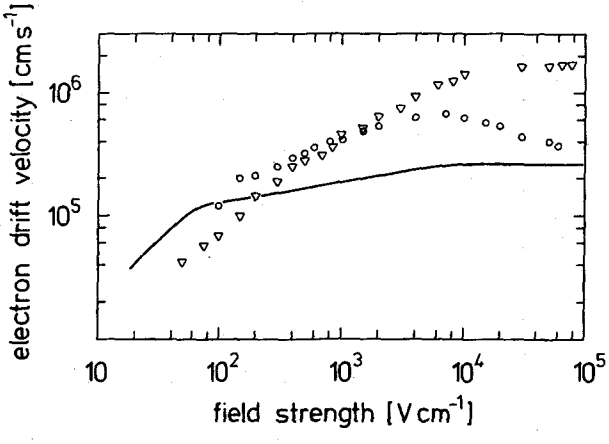

Fig. 7: Influence of butane on the drift velocity of electrons in liquid xenon; ○ 1.26 10^{19} cm^{-3}; ▽ 1.9 10^{20} cm^{-3} ; T (Xe) 165 K [30]

were observed [21]. At low electric field strength, a low mobility characteristic of electron bubbles was measured. At high electric fields, a fast electronic signal was observed which gave drift velocities characteristic of delocalized electrons.

In the heavier liquefied rare gases, the mobility depends on temperature in a complicated fashion (see Fig. 5).

The electron drift velocity in lAr, lKr, and lXe increases sub-proportionally with electric

field strength (see Fig. 6), or in other words, the electron mobility decreases with the electric field strength. Such a behavior is interpreted by an increase of the mean electron energy due to pick-up of energy from the applied electric field. At 10^5 V/cm, the mean energy is of the order of 1 eV. Addition of nitrogen gas leads to an increase of the saturation drift velocity. The nitrogen molecule can absorb electron energy through the excitation of vibrations.

The addition of small amounts of butane to liquid xenon influences the electron transport properties in a distinctive way. Small amounts of solute first increase of the value of the drift velocity with electric field above the values of the pure xenon ($\leq 10^4$ V/cm). With further increase of the field strength, the drift velocity approaches the saturation velocity of pure xenon. The larger concentration of butane reduces the low field mobility due to scattering of thermal electrons and it leads to a higher saturation drift velocity at high fields due to more effective cooling of the hot electrons (see Fig. 7).

The high electron mobility of lAr, lKr, and lXe makes these liquid suitable as ionization media in liquid ionization chambers, operating in the electron pulse mode. Here, the current signal induced by the motion of highly mobile electrons in an applied electric field can be amplified and processed by electronic amplifiers, counters, and pulse height analyzers, which are usually used with solid state radiation detectors. Because of its low price, lAr has found large scale applications in detectors of high energy particle physics. The use of liquids allows the design of special electrode geometries of the ionization chamber.

8. Ions

Liquefied rare gases represent ideal matrices for the study of ions in an inert condensed phase. The atoms can be considered as polarizable spheres. The main effect to be considered is that of electrostriction which leads to an increase of density of the liquid around the ion. This clustering leads to an increase of radius and mass of the ion and it results in a lower diffusion coefficient of the ion as compared to the neutral rare gas atom. There are differences of this effect for positive and negative ions due to the fact that for a negative ion the lone electron is repelled by the closed shells of the rare gas atoms comprising the liquid. Theoretical studies have been carried out and are continuing in order to understand the influence of this repulsion on the electrostriction in more detail [31], [32]; [33].

9. Radiation Detectors with Liquids

The electron pulse signal produced by a track of ionizing radiation traversing the liquid gap of a parallel plate ionization chamber depends on the orientation of the track with respect to the field. In order to measure the total electron charge produced in the track of a particle or quantum of an arbitrary orientation with respect to the electric field lines, a grid may be inserted close to the anode into the electrode gap (see Fig. 8, Frisch grid). The electron signal is measured between the grid and the anode. All electrons entering into the grid/anode space are then detected. The transmission of the ionization electrons through the grid depends on the separation of the grid wires and on the field strength in the grid/anode gap [34].

Electron pulse chambers have found many applications, especially in high energy physics. Here, calorimeters filled with lAr, lKr, or lXe have been developed.

In a calorimeter, the total energy expended in all particles originating from the interac-

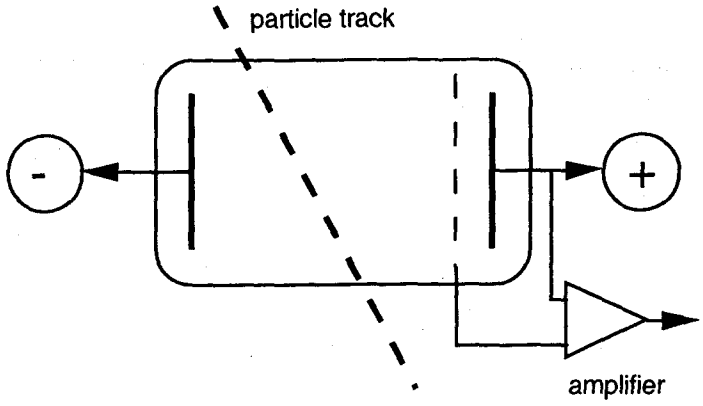

Fig. 8: Liquid ionization chamber with Frisch grid

tion of two energetic elementary particles is measured. The most widely used calorimeter consists of absorber plates made of some heavy metal (lead, iron, uranium) intercalated with thin liquid ionization chambers filled with liquid argon. The ionization chambers operate at high electric field strength where the electron drift velocity approaches its saturation value of v_s=6.4 10^5 cm/s. The time resolution is limited by the specific drift time of v_s^{-1}=1.56 μs/cm. The principle of a sandwich calorimter is shown in Fig. 9.

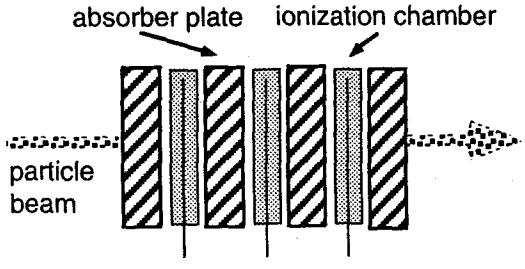

Fig. 9: Principle of a sandwich calorimeter

Calorimeters based on liquid xenon or liquid krypton do not require absorber plates due to the higher density of lXe or lKr. The particles lose their energy entirely in the liquid volume. With segmented electrodes the total charge produced by absorption of an individual particle can be measured.

Liquid xenon exhibits the highest electron mobility of all RGLs and at sufficiently high electric field strengths electron avalanches may occur. An example is shown in Fig. 10, where the electron current produced by an alpha source on the cathode of a diode cell immersed in lXe is shown as a function of the applied electric field strength.

This liquid is especially suited as detection medium in a proportional counter [36]. Very fine anode wires (diam. $\leq$ 5 μm) are required in order to avoid spurious pulses produced at inhomogeneities found on the surface of thicker wires.

One of the promising imaging devices to be employed in high energy physics research is the liquid-argon time projection chamber (TPC) [37] ; [38]. A high energy particle creates a track of ionization events in the liquid consisting of fast electrons and slow positive ions. The electrons represent an image of the path of the high energy particle. Under the influence of an applied electric field the electrons drift towards the anode which constists of two perpendicular sets of wires (see Fig. 11). Each wire is connected to a charge sensitive amplifier. From the drift time, t_d, the z-coordinate, and from the wires, the x- and y-coordinates are

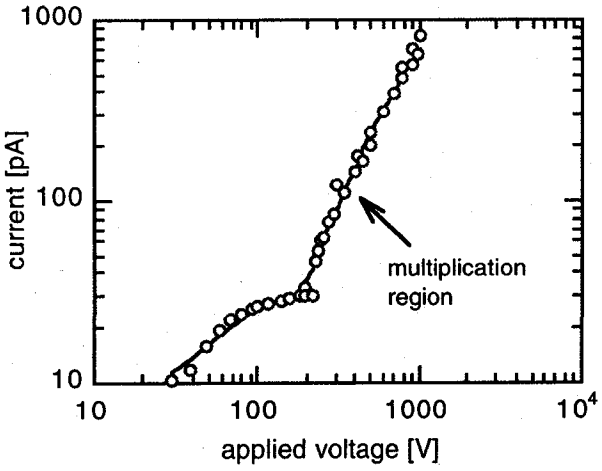

Fig. 10: Electron current in a diode cell with a radioactive alpha source on the cathode [35]

obtained. This way, a three-dimensional image of the track can be reconstructed. Very pure liquid is necessary in order to avoid loss of electrons due to attachment.

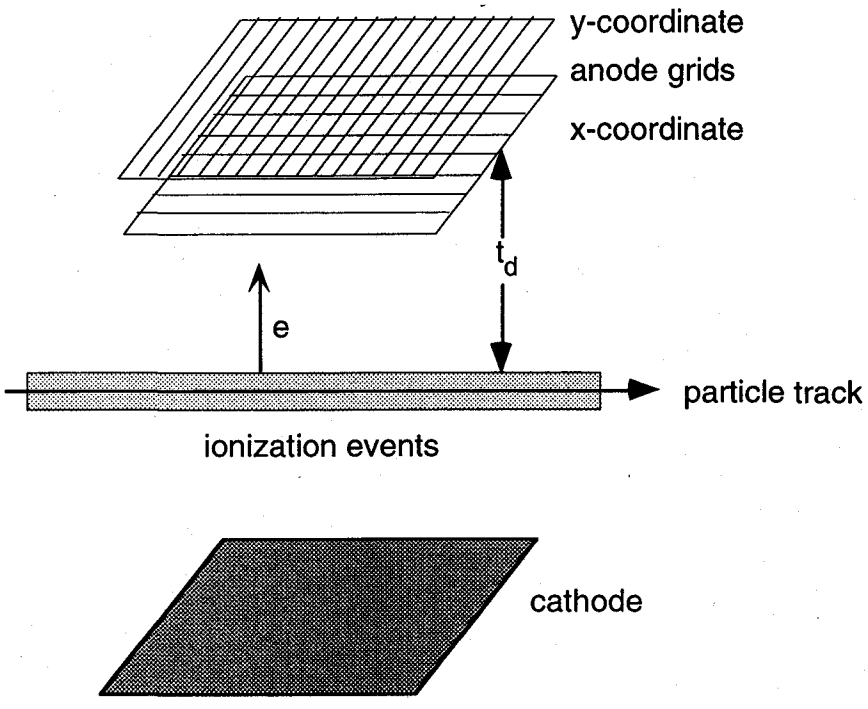

Fig. 11: Principle of the time projection chamber

Since several years, the construction of a very big TCP is under way in Italy under the leadership of Carlo Rubbia. This detector, initially called ICARUS, will eventually contain several kilotons of liquid argon. It is placed underground in a cave in the Grand Sasso Massiv where it is to detect strange particles from outer space. The design principle has been tested with 3 tons of lAr, and the construction of a 600 ton module is under way.

The purification and handling of such large quantities of RGLs represents a qualitatively different task as compared to laboratory style of preparation.

A standard instrument in high energy physics experiments is the liquid argon calorimeter with absorber plates from heavy metals (iron, lead, uranium). The liquid ionization chambers, usually, have electrode separations of 1 or 2 mm and operate at field strengths of several kV/cm. This leads to electron collection times in the sub-microsecond time domain [39];

[40]. Liquid argon of sufficient purity (oxygen impurity level approximately 1ppm) from a storage tank is evaporated and re-condensed in to the calorimeter. No additional purification is necessary. In the case of TCPs, drift distances of up to 1.5 m are envisaged which require a purity of the argon of less than 1 ppb impurities.

In medical radiology, many different detectors are necessary. Since the beginning of radioscopy, for the imaging of the attenuation of the x-rays the photographic film is used. Modern methods use semiconductor arrays. Another possibility represents the gamma-camera filled with high pressure xenon gas or liquid xenon. The digitization of the image is effected by two sets of electrode strips which are placed perpendicular to each other with a small distance between them. Each crossing point represents a small ionization chamber in which the local x-ray intensity is measured. The principle is schematically depicted in Figure 12.

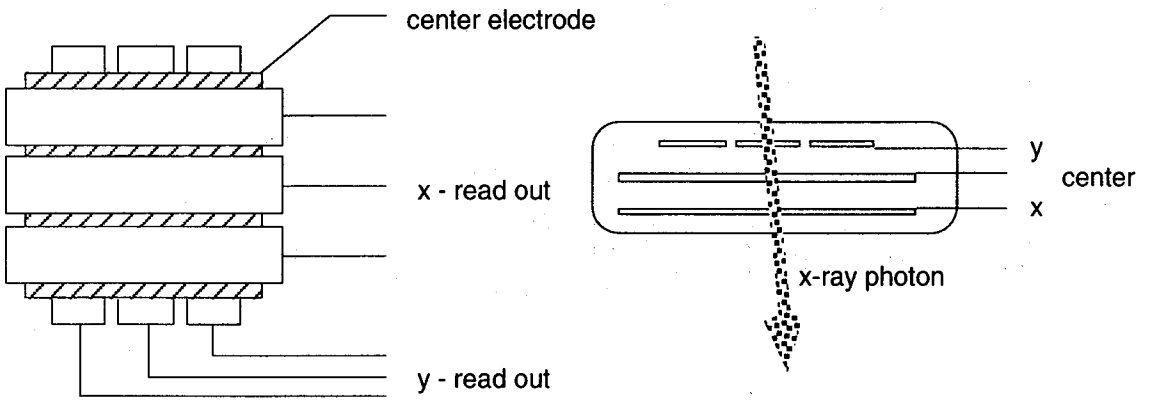

Fig. 12: Principle of a position sensitive detector (gamma camera)

In high pressure gamma cameras, the strips may be replaced by wires and electron avalanches near the wires represent an internal amplification.

10. Ultrapurification of Cryogenic Rare Gas Liquids

The main molecular impurities in the rare gases are the following: **Oxygen, Nitrogen, Hydrogen, Carbon dioxide, Hydrocarbons, Water**

Depending on the level of purity their concentration is in the ppm (parts per million) range. In addition, neon, argon, krypton and xenon contain small concentrations (in the range of 1 to 10 ppm) of the other rare gases. For instance, xenon contains krypton and argon, neon contains helium and argon.

For the use in radiation detectors operating in the electron pulse mode, removal of all electron attaching impurities is mandatory. Metal getters or large surface area materials as silicagel or molecular sieves have been employed. A number of purifiers are commercially available. Those employing metal getters operate at higher temperatures.

A simple effective way to remove oxygen and other electron attaching impurities is to pass the gas over a titanium sponge held at 700℃. This metal also reacts with nitrogen and removes it from the rare gas. In another method, titanium electrodes in a discharge chamber are used. The discharge disperses the titanium as small particles which adsorb the impurities. For the purification of small amounts of gas, barium getters or hot calcium chips can be employed.

The purification of larger quanitites of gas (> 1 liter of liquid) can be done by the use of non-evaporable metal getters, consisting of zirconium, vanadium and iron. The ingots are activated at a higher temperature (400 to 500℃) and their operating temperature is between 200 and 300℃. All connecting tubes and vessels should be made of stainless steel. For electrical feedthroughs, ceramic material is used. In order to clean the inner surfaces of the experimental equipment, the gas is cirulated for several hours through the detector and the purifier.

For the purification of very large liquid quantities of argon (> 1 ton of liquid), a purification system employing large filters containing molecular sieves and silicagel was developed [41]. A schematic of the liquid purification system is shown in Fig. 13.

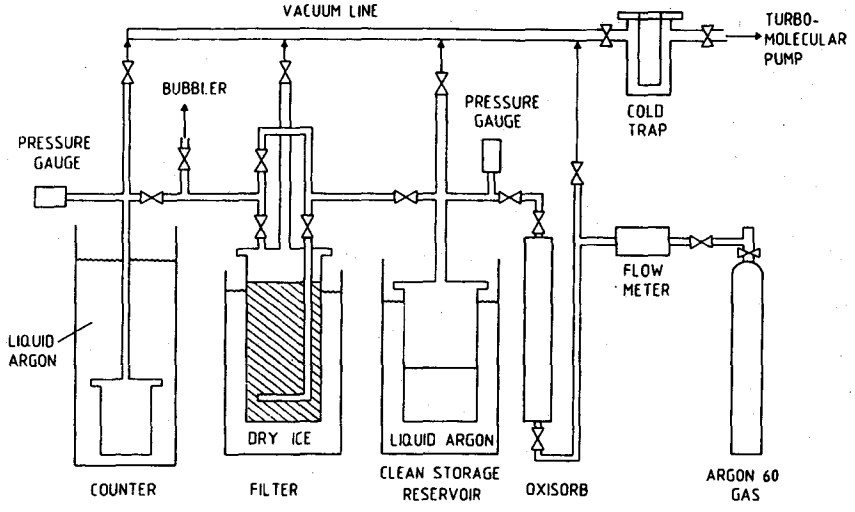

Fig. 13: Schematic of an argon purification system developed at CERN, Switzerland [41]

The filter consisted of an equal mixture of molecular sieves 4Å and 13X and of silicagel. The filter was activated by pumping on it at 350℃ for several days until the pressure had dropped to 10^{-5} mbar. The filter was then kept at dry ice temperature during the purification of the tank argon gas. In order to remove the oxygen a high surface area room tmperature getter was used (commercial name Oxisorb) The Oxisorb cartridge is made of cromium embedded in a SiO_2 lattice. The oxygen is chemically removed via the reaction $2Cr + 3\ O_2 \rightarrow 2\ CrO_3$. With this method, liquid argon could be obtained which had a rest level of oxygen of 0.03 ppb (parts per billion).

An alternative way in large scale purification is the passage of the liquid phase through filters with active getters. In the development of a lKr calorimeter (> 20 tons) The liquid was pumped continuously through an Oxysorb cartridge of sufficient capacity [42].

The removal of hydrocarbons, which may be important for other applications, is more difficult. Generally, the best way is the destruction of the hydrocarbons either by an electrical discharge or by irradiation with gamma-rays [43].

11. Conclusion

Ultrapure liquefied rare gases have gained importance as ionization media in radiation detectors. The information on rare gas purification gained from the development of these detectors will lead to further applications of RGLs in other areas of science and technology. Espe-

cially, liquid xenon has a great potential as an inert solvent in many laboratory and industrial processes.

References

[1] Air Liquide. *Gas Encyclopaedia.* . 1976, Elsevier: Amsterdam.

[2] Rentzepis, P.M. and Douglass, D.C. *Xenon as a solvent.* Nature. 1981. **293**: p. 165-166.

[3] Crawford, R.K., *Melting, Vaporization and Sublimation.* in *Rare gas solids.* M.L. Klein and J.A. Venables, Editors. 1977, Academic Press: London, New York, San Francisco. p. 663-728.

[4] Hammarlund, N. *The krypton and xenon markets up to the year 2000.* Nuclear Instrum. Meth. 1992. **A316**: p. 83-87.

[5] Stratton, J.A. *Electromagnetic theory.* International series in pure and applied physics. ed. L.I. Schiff. 1941. New York, London: McGraw-Hill Book Co

[6] van der Elsken, J., van Zoonen, P., and Michielsen, J.C.F. T*he non-linear dielectric effect in liquid xenon.* Chem. Phys. Lett. 1984. **106**(**4**) : p. 252-257.

[7] van der Elsken, J. and Michielsen, J.C.F. *The non-linear dielectric effect in xenon. The density dependence.* Chem. Phys. Lett. 1985. **115**(2) : p. 230-235.

[8] Bokov, O.G. and Naberukhin, Y.I. *Application of the Onsager model to the theory of the dielectric constant of nonpolar liquids.* J. Chem. Phys. 1981. **75**: p. 2357-2365.

[9] Cockett, A.H. and Smith, K.C., *The monatomic gases: Physical properties and production.* in *Comprehensive inorganic chemistry.* J.C. Bailar, *et al.*, Editor^Editors. 1973, Pergamon Press: Oxford, New York, Toronto. p. 139-211.

[10] Rechowicz, M. *Electric power at low temperatures.* Monographs in electrical and electronic engineering. ed. P. Hammond and D. Walsh. 1975. Oxford: Clarendon Press.

[11] Gee, N., *et al. Dielectric constant against temperature for 43 liquids.* J. Chem. Thermodynamics. 1986. **18**: p. 221-234.

[12] Landolt-Bornstein. *Statische Dielektrizitatskonstanten reiner Flussigkeiten und binarer flussiger Mischungen.* Zahlenwerte und Funktionen aus Naturwissenschaften und Technik. ed. O. Madelung. Vol. 6. 1991. Springer-Verlag: Berlin, Heidelberg, New York.

[13] Miller, L.S., Howe, S., and Spear, W.E. *Charge transport in solid and liquid Ar, Kr, and Xe.* Phys. Rev. 1968. **166**: p. 871-878.

[14] Rademann, K. *Photoionization mass spectrometry and valence photoelectron- photoion coincidence spectroscopy of isolated clusters in a molecular beam.* Ber. Bunsenges. Phys. Chem. 1989. **93**: p. 653-670.

[15] Haberland, H., *et al. Experimental study of the transition from van der Waals over covalent to metallic bonding in mercury clusters.* J. Chem. Soc. Farad. Trans. 1990. **86**: p. 2473-2483.

[16] Gubanov, A.I. *Quantum electron theory of amorphous conductors.* 1965. New York: Consultants Bureau.

[17] Schmidt, W.F. *Liquid state electronics of insulating liquids.* 1997. Boca Raton: CRC Press.

[18] Born, M. *Volumen und Hydratationswarme der Ionen.* Z. Physik. 1920. **1**: p. 45-48.

[19] Martin, T.L. and Leonard, W.F. *Electrons in crystals.* Brooks/Cole electrical engineering series. ed. T.L. Martin. 1970. Belmont, California: Brooks/Cole Publ. Co. 705.

[20] Nelson, D.A. and Ruoff, A.L. *Metallic xenon at static pressures.* Phys. Rev. Lett. 1979. **42**(6) : p. 383-386.

[21] Sakai, Y., Schmidt, W.F., and Khrapak, A.G. *High- and low-mobility electrons in liquid neon.* Chem. Phys. 1992. **164**: p. 139-152.

[22] Schmidt, W.F. *Electronic conduction processes in dielectric liquids.* IEEE Trans. Electr. Insul. 1984. **19**: p. 389-418.

[23] Spear, W.E. and LeComber, P.G., *Electronic transport properties. in rare gas solids.* M.L. Klein and J.A. Venables, Editor^Editors. 1977, Academic Press: London, New York, San Francisco. p. 1120-1149.

[24] Schwarz, K.W. *Charge-carrier mobilities in liquid helium at the vapor pressure.* Phys. Rev. 1972. **A6**(2) : p. 837-844.

[25] Bruschi, L., Mazzi, G., and Santini, M. *Localized electrons in liquid neon.* Phys. Rev. Lett. 1972. **28**: p. 1504-1506.

[26] Sakai, Y., Bottcher, E.H., and Schmidt, W.F. *Excess electrons in liquid hydrogen, liquid neon, and liquid helium.* J. Electrostatics. 1982. **12**: p. 89-96.

[27] Sakai, Y., Bottcher, E.H., and Schmidt, W.F. *High field electronic conduction in cryogenic liquids (in Japanese).* J. Japan. Inst. Electr. Eng. 1983. A61: p. 499-506.

[28] Gushchin, E.M., Kruglov, A.A., and Obodovskii, I.M. *Electron dynamics in condensed argon and xenon. Sov.* Phys. JETP. 1982. **55**(4) : p. 650-655.

[29] Kimura, T. and Freeman, G.R. *Band-Nonband mobility transitions for extra electrons in liquid xenon.* Can. J. Phys. 1974. **52**: p. 2220-2222.

[30] Yoshino, K., Sowada, U., and Schmidt, W.F. *Effect of molecular solutes on the electron drift velocity in liquid Ar, Kr, and Xe.* Phys. Rev. 1976. **A14**(1) : p. 438-444.

[31] Hilt, O., Schmidt, W.F., and Khrapak, A.G. *Ionic mobilities in liquid xenon.* IEEE Trans. Dielectrics Electr. Insul. 1994. **1**: p. 648-656.

[32] Volykhin, K.F., Khrapak, A.G., and Schmidt, W.F. *Structure and mobility of negative ions in dense gases and non-polar liquids.* JETP. 1995. **88**(2) : p. 320-324.

[33] Yoshino, K., *et al. Structure and energy spectrum of negative ions in non-polar liquids.* in *ICDL 2002.* 2002. Graz: IEEE.

[34] Bunemann, O., Cranshaw, T.E., and Harvey, J.A. *Design of grid ionization chambers.* Can. J. Res. 1949. **27**: p. 191-206.

[35] Yoshino, K., Sowada, U., and Schmidt, W.F. *High field electron transport in liquids.* Technol. Repts. Osaka Univ. 1977. **27**: p. 145-157.

[36] Miyajima, M., *et al. Proportional counter filled with highly purified liquid xenon.* Nucl. Instrum. Methods. 1976. **134**: p. 403-405.

[37] Rubbia, C. *The liquid-argon time projection chamber: A new concept for neutrino detectors.* . 1977, CERN.

[38] Mahler, H.J., Doe, P.J., and Chen, H.H. *Operation of a liquid argon time projection chamber.* IEEE Trans. Nucl. Sci. 1983. **NS-30**: p. 86-89.

[39] Fabjan, C.W., *Calorimetry in high energy physics.* in *Techniques and concepts of high-energy physics.* T. Ferbel, Editor^Editors. 1985, Plenum Publishing Corporation: New York.

[40] Engler, J. *Status and perspectives of liquid argon calorimeters.* Nucl. Instrum. Methods. 1984. **225**: p. 525-529.

[41] Buckley, E., *et al. A study of ionization electrons drifting over large distances in liquid argon.* Nucl. Instrum. Methods. 1989. **A275**: p. 364-372.

[42] Schinzel, D. *The Kr-calorimeter,* private communication 1996.

[43] Hilt, O. *Elektronische und ionische Leitungsprozesse in flussigem Xenon.* 1995. Aachen: Verlag Shaker.